

# Structure and physical properties of the bipolar outflow source NGC 7023

G. D. Watt<sup>1</sup>, W. B. Burton<sup>2</sup>, S.-U. Choe<sup>3</sup> and H. S. Liszt<sup>4</sup>

<sup>1</sup> Radiosterrenwacht, Postbus 2, NL-7990 AA Dwingeloo, The Netherlands

<sup>2</sup> Sterrewacht, Postbus 9513, NL-2300 RA Leiden, The Netherlands

<sup>3</sup> Dept. of Earth Science, College of Education, Seoul National University, Seoul 151, Korea

<sup>4</sup> National Radio Astronomy Observatory, Charlottesville, VA 22901, USA

Received December 26, 1985; accepted April 8, 1986

**Summary.** The reflection nebula NGC 7023 has been mapped in both the  $^{12}\text{CO}$  and  $^{13}\text{CO}$   $J=1-0$  transitions. The region displays features characteristic of an outflow source with outflowing lobes directed along the minor axis, i.e. direction of least resistance, of a much longer low density molecular cloud. There is little indication from the spectra of high velocity wings arising from material within the outflowing lobes, but dense CO regions are found at the ends of the flows where the interaction with the ambient cloud has resulted in compression and heating. Optical depths, excitation temperatures, and column densities are calculated from the data and a geometrical model is constructed to fit the observed and derived parameters. Momentum and energy in the flows are consistent with values from other bipolar sources and constitute 0.6% of the radiative energy available from the exciting source, in this case a B3 star. The emission structure evident around the star is interpreted as the heated inner surface of a cavity created by the Strömrgren shell as the star evolved.

**Key words:** interstellar medium: clouds: individual – interstellar medium: reflection nebulae: individual – stars: formation of

## 1. Introduction

The reflection nebula designated NGC 7023 and its associated star HD 200775 have been the subject of several studies in the optical and ultraviolet wavelengths. Reviews and references to earlier publications are found in Johnson (1965) and in Vanysek (1969). Van Houten (1961) discussed a model for the nebula involving a small H II region surrounding the exciting star HD 200775 (see Witt and Cottrell, 1980a) which is most likely a newly formed star of less than  $10 M_{\odot}$  with a dust cocoon (Ney et al., 1980). Combined UV, optical, and IR observations (Altamore et al., 1980) provide further evidence for an extended shell of dust and gas around this star, which is evidently a typical early type B star. The infrared emission is consistent with thermal emission from dust at  $\sim 3 \cdot 10^{14}$  cm radius (Whitcomb et al., 1981); this shell may interact with the surrounding nebula producing OH emission (Lépine and

Nguyen-Quang-Rieu, 1975). Radio line observations have been made by Pankonin and Walmsley (1978) of C 158 $\alpha$ , C 110 $\alpha$ , OH (1667 MHz), and H<sub>2</sub>CO from the position of HD 200775. CO detections were made by Loren et al. (1973), Kutner et al. (1980), and Myers et al. (1983); extensive low resolution mapping was done by Elmegreen and Elmegreen (1978) and by Elmegreen (1982) who also detected the  $^{13}\text{CO}$  isotope and CS emission.

NGC 7023 appears quite prominent on the Palomar Sky Survey photographs lying about  $14^{\circ}$  distant from the galactic plane at  $l=104^{\circ}$  in a region generally free from other nebulosity. The central illuminating object is classed as a Be 3 IV-V dwarf emission star at an estimated distance of 440 pc (Mendoza, 1955; Viotti, 1969) or of 350 pc (Witt and Cottrell, 1980). This star is the centre of a  $T$  association containing some 14 stars including LkH $\alpha$  275, 276, 427, as well as several irregular variables, and 6 far-IR emitters (Gezari et al., 1984). The total mass of this cluster is estimated at about  $100 M_{\odot}$ .

The CO ( $J=1-0$ ) mapping reported here covers an area  $\frac{1}{2}^{\circ} \times 1^{\circ}$ . It indicates a large extended cloud, with a higher-density clump at the northern end in which two peaks of emission are found adjacent to a “hole” in the optical extinction. The proper motions of the stars in the “hole” have been observed by Weston (1953), who found that the group is not physically related but appears as a cluster due to a gap in the obscuring material.

## 2. CO observations

The  $J=1-0$   $^{12}\text{CO}$  and  $^{13}\text{CO}$  observations presented here were made with the 36-foot antenna of the NRAO in two runs during 1980 and 1981. At these line frequencies the half-power beamwidth of the telescope is approximately  $1'$ . Integration times of about 8 min resulted in  $3\sigma$  noise levels of 0.4 K at our spectral resolution 250 kHz or  $0.67 \text{ km s}^{-1}$ . The CO intensities discussed here are in terms of  $T_A^*$  as defined by Kutner and Ulrich (1981).

## 3. CO results

Figures 1 and 2 display, for  $^{12}\text{CO}$  and  $^{13}\text{CO}$  respectively, maps of peak corrected antenna temperature, mean velocity, half power

Send offprint requests to: G. D. Watt

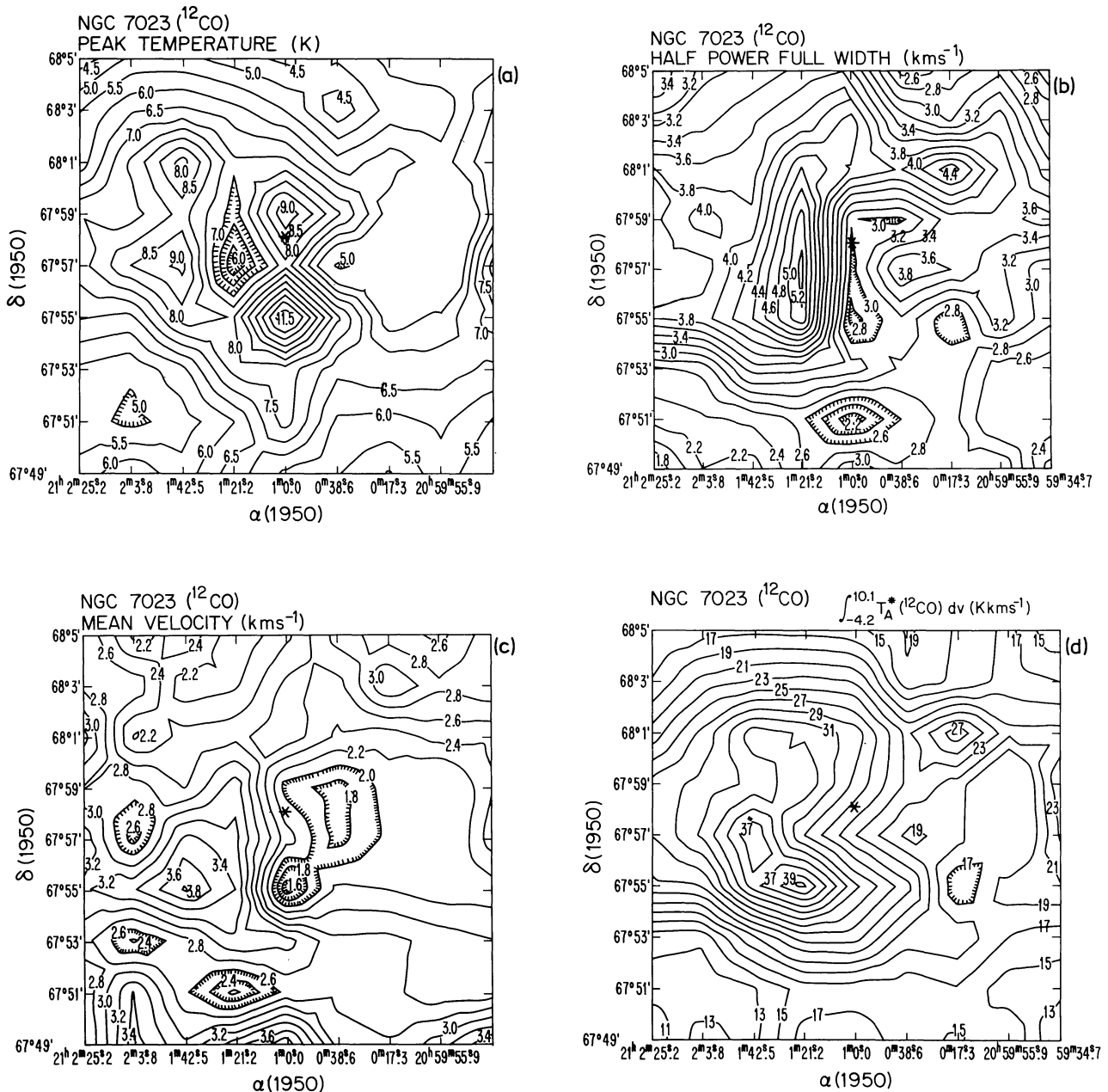


Fig. 1a–d. Maps of peak antenna temperature, mean velocity, half-power full line width, and integrated antenna temperature for the  $^{12}\text{CO}$  line observed in the vicinity of NGC 7023

full linewidth and integrated antenna temperature. The  $^{12}\text{CO}$  data shows several of the features typical of a bipolar source, such as intense emission surrounding the central star, outflowing lobes projected in opposite directions centred on the star, and the detection of velocity structure and intensity variations along the lobes. The exciting star HD 200775 is represented on each diagram by an asterisk. Figure 1a shows a ridge of emission lying in a north-south direction across the exciting object with intensity peaks at each end. Such a distribution suggests a region of high-excitation lying roughly perpendicular to the outflow lobes which may help to confine the high velocity flow, may be the source of the outflow, or may be a result of some of the original cloud material untouched by the outflow which has been collimated at a smaller circumstellar

radius. The  $^{13}\text{CO}$  emission, a better indicator of density than the more abundant  $^{12}\text{CO}$  isotope, does not show a ridge (see Fig. 2a) but does have emission maxima on either side of the exciting star. There is a shift in the mean velocity of both species (noticeable more clearly in Fig. 3a) from north to south across the ridge of about  $1.0 \text{ km s}^{-1}$ . Towards the east of HD 200775 is a dip in the  $^{12}\text{CO}$  peak intensity followed by an increase in emission more clearly observed in  $^{13}\text{CO}$ , a rapid increase in the linewidth of both species, and a systematic mean velocity shift by  $\sim 2 \text{ km s}^{-1}$  towards the red (see Fig. 3b). The Palomar Sky Survey photographs show that this feature is connected to the crossing of an ionization band visible on both red and blue plates. Beyond the ionization front a fainter north-south ridge of  $^{12}\text{CO}$  emission is

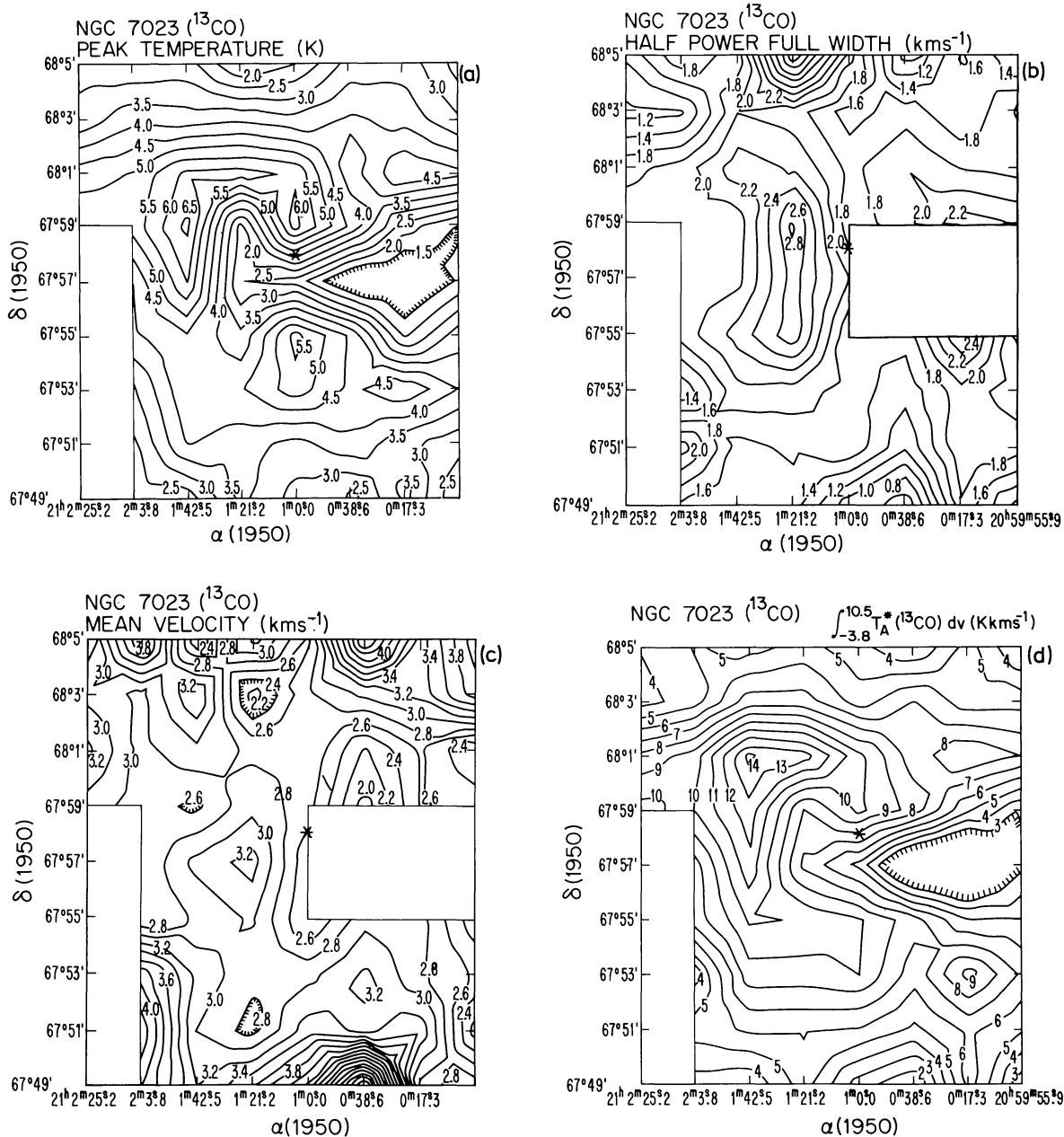


Fig. 2a–d. Maps of peak antenna temperature, mean velocity, half-power full line width, and integrated antenna temperature for the  $^{13}\text{CO}$  line observed in the vicinity of NGC 7023

detected (Fig. 1a) with maxima at each end. The  $^{13}\text{CO}$  map peaks between these maxima (Fig. 2a).

The maps of integrated antenna temperature (Figs. 1 and 2d) both show an arc of emission to the east of HD 200775 which in  $^{12}\text{CO}$  peaks towards the south but in  $^{13}\text{CO}$  peaks toward the north. Taking the various excitation parameters into consideration it appears likely that there is a higher temperature clump toward the south and a higher density clump toward the north. Toward the west of HD 200775 the  $^{13}\text{CO}$  spectra are weak and certain parameters are not determinable, hence the blank areas in Fig. 2. The  $^{12}\text{CO}$  emission shows a hole extending nearly to the edge of our mapped area but also indicates a rise in intensity at the western edge of the map. This rise is the edge of the other outflow lobe

which appears on the map of Elmegreen and Elmegreen (1978) but which unfortunately was not included in our mapping. The region of very low emission corresponds to the optical hole visible on the POSS plates. There also appears to be a secondary peak in integrated emission from both species towards the north of the hole.

NGC 7023 therefore shows the signature of a bipolar outflow source, with two lobes lying roughly NE-SW and a region of excited material surrounding the central star approximately perpendicular to the lobes. The eastern lobe is shorter than the western one, and shows evidence for an ionization front and a ridge of dense material. The western lobe extends across an optical hole in the cloud. We suggest that the eastern lobe represents red-shifted

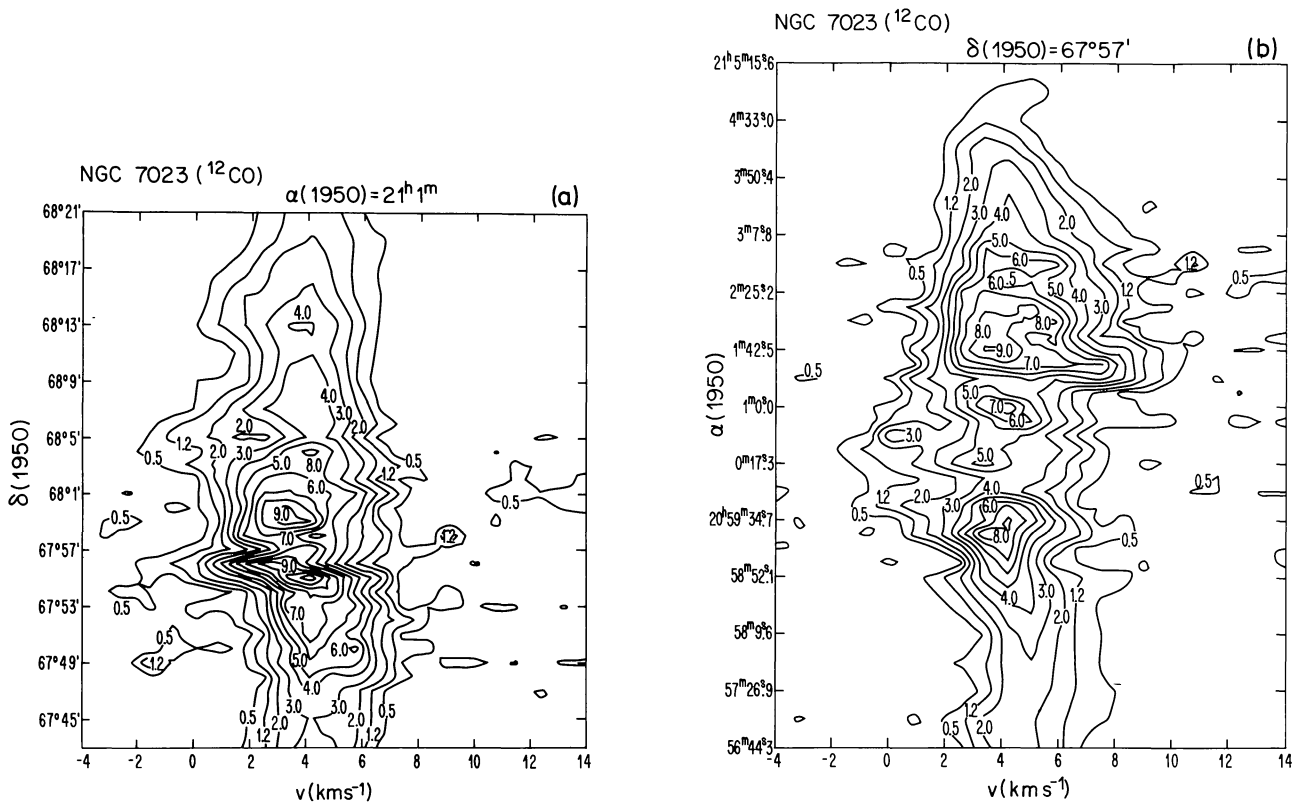


**Fig. 3a and b.** Position-velocity maps of  $^{12}\text{CO}$  intensities plotted against declination (a) and against right-ascension (b) through the position of the exciting star HD 200775. The contours are labeled in degrees K. **a** shows the extent of the molecular cloud in the north-south direction, and the  $1 \text{ km s}^{-1}$  velocity shift centered on the position of the exciting star. **b** shows the geometry of the region in a more favourable orientation; it shows the enhanced emission from the eastern and western lobes, as well as the higher velocity dispersions there, the deficiency of CO emission from the region of the optical hole, and enhanced emission from the small central region

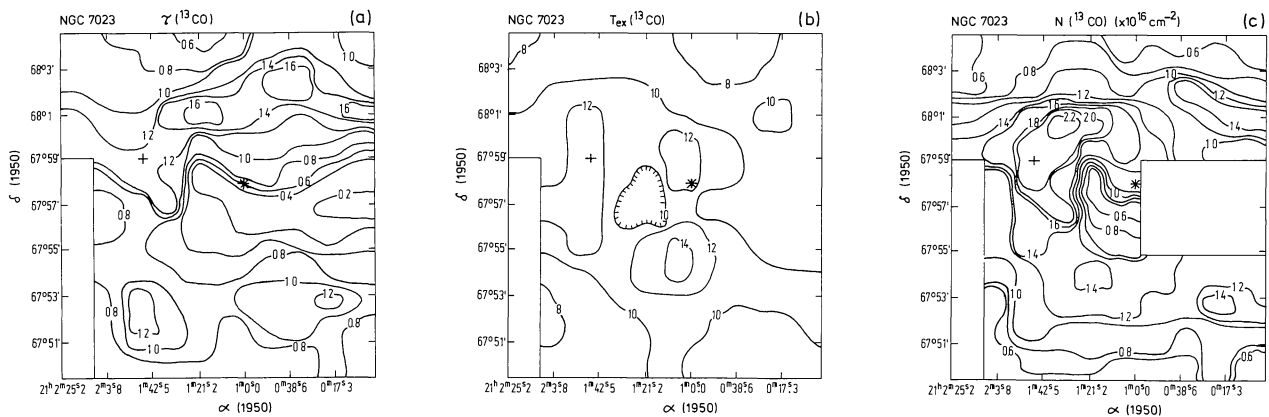


**Fig. 4a–c.** Derived properties of the eastern lobe. **a** The opacity in the  $^{13}\text{CO}$  line shows a general deficiency in the direction of the exciting star. **b** The  $^{13}\text{CO}$  excitation temperature shows maxima on either side of the central star and a minimum in the region of outflow. **c** The  $^{13}\text{CO}$  column density shows a peak in the north-east which we interpret as the end of outflow-lobe; the symmetric south-east region occurs where the  $^{13}\text{CO}$  intensities are too weak to allow reliable determination of profile widths. The position of the exciting star is indicated by a “\*”: the position of the CS detection is indicated by a “+”

emission travelling into the front surface of a molecular cloud and that the western lobe represents blue-shifted emission possibly expanding out from the edge of the cloud. The weak appearance of the velocity structure in the western lobe (Fig. 3b) may be a result of the density dropping at the edge of the cloud which effectively reduces the  $^{12}\text{CO}$  usefulness in tracing the flow.

Figure 3a shows a declination velocity plot for a line of constant right ascension crossing HD 200775 at  $\alpha(1950) = 21^{\text{h}}01^{\text{m}}00^{\text{s}}$ . Here the velocity shift of  $\sim 1 \text{ km s}^{-1}$  across the disk is seen, as is the extent of the molecular cloud in a N-S direction. Figure 3b is a right ascension velocity plot through  $\delta(1950) = 67^{\circ}57'00''$  showing the two lobes of emission. This strip map shows a larger extent than

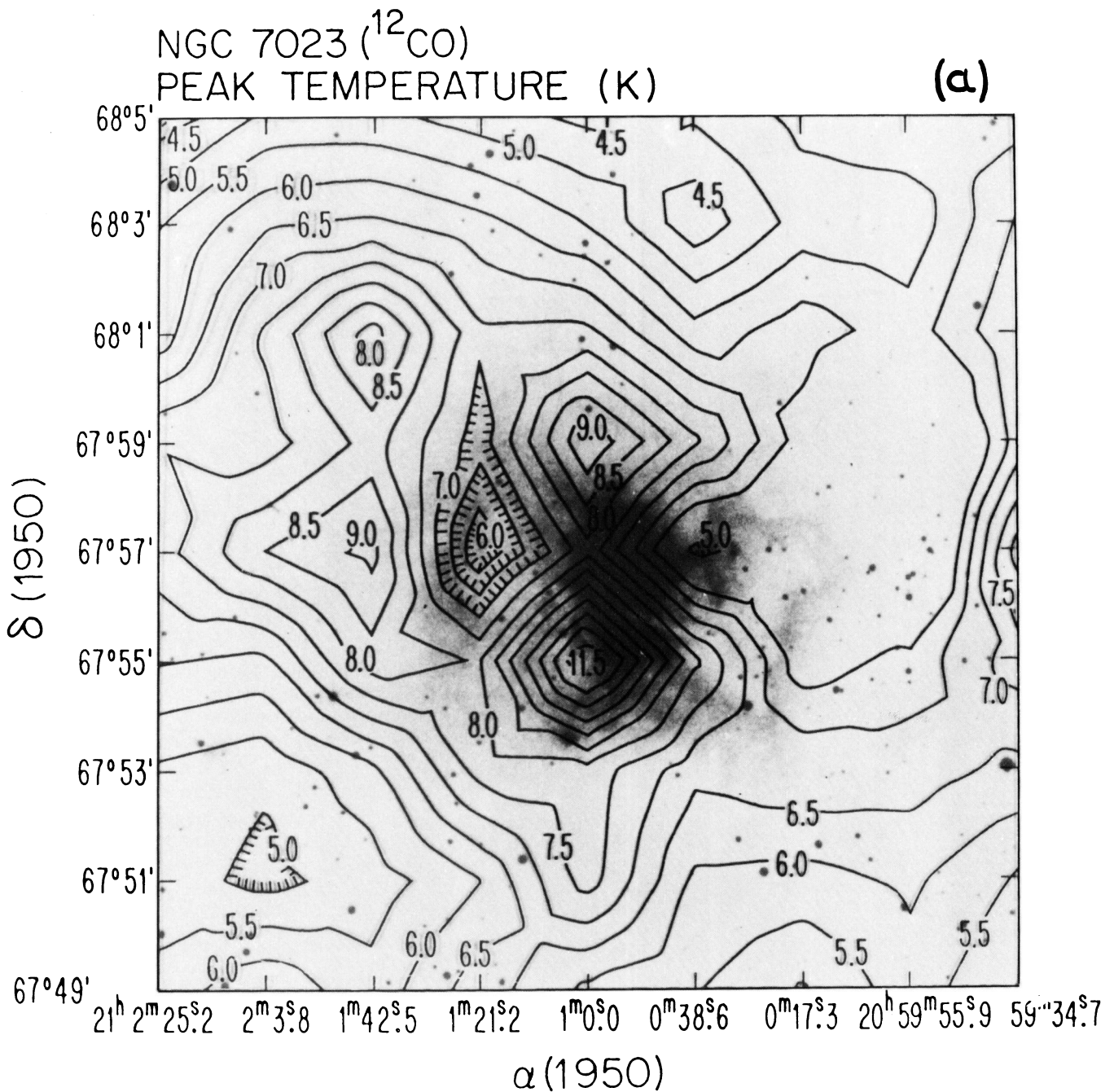


Fig. 5a. Peak  $^{12}\text{CO}$  antenna temperature superimposed on the red POSS plate of NGC 7023

that of the area mapped in two dimensions. It shows the eastern lobe with its western edge exhibiting a large velocity dispersion as the ionization ridge is crossed. Some emission is present at the central location; the western lobe emission is also extended but does not show any large dispersion due to any ionization fronts. The emission from the central position does not suggest the presence of the high velocity gas characteristic of most bipolar sources, although most of our spectra were not of adequate signal-to-noise to investigate the line wings. It should be stressed that our evidence for the existence of the outflow lobes hinges on the detection of the two clumps of gas at the ends of the outflows.

Because the western lobe was not covered by our mapped area, further analysis is restricted to the eastern lobe and the central high-excitation region.

Figure 4 illustrates the properties of the eastern lobe. Figures 1a and 2a show that the peak antenna temperatures in the lobe zones are  $T_A^*(^{12}\text{CO}) = 8.5$  K and  $T_A^*(^{13}\text{CO}) = 6.0$  K. The opacity is calculated in the standard manner assuming that the excitation temperatures of  $^{12}\text{CO}$  and  $^{13}\text{CO}$  are equal and that  $\tau_{12} \gg 1$ . Then

$$\tau_{13} = -\ln \left[ 1 - \frac{T_A^*(^{13}\text{CO})}{T_A^*(^{12}\text{CO})} \right],$$

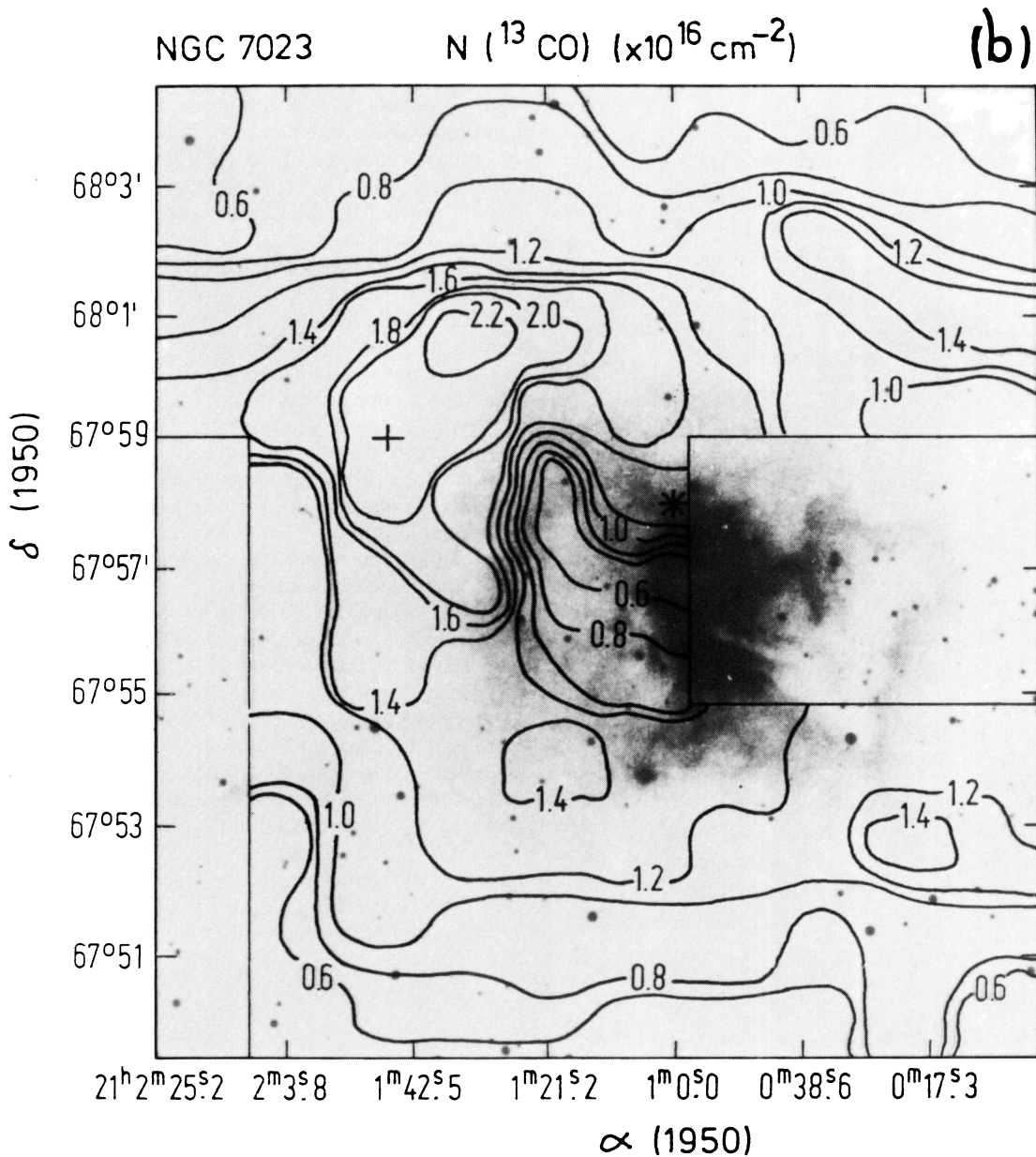


Fig. 5b. Column density of  $^{13}\text{CO}$  superimposed on the red POSS plate

which leads to a resulting optical depth between 1 and 2 in the N and NE with a couple of clumps of  $\tau \gtrsim 1$  in the south. The excitation temperature of  $^{13}\text{CO}$  follows from

$$T_{\text{ex}}(^{13}\text{CO}) = \frac{h\nu}{k} \left\{ \ln \left[ 1 + \frac{h\nu}{k(T_A^*(^{12}\text{CO}) + T_{bg})} \right] \right\}^{-1}$$

where  $h\nu/k = 5.54$  for  $^{13}\text{CO}$  and  $T_{bg}$  is the contribution to the intensity from the cosmic background radiation ( $T_{bg} = 0.817$  K) at the frequency  $\nu$ . Figure 4b shows the ridge of high excitation temperature to the NE, maxima on either side of the central star, and a dip within the outflowing lobe. The column density of  $^{13}\text{CO}$  is thus a function of the two previously determined parameters.

$$N(^{13}\text{CO}) = \frac{2.31 \cdot 10^{14} \tau_{13} \Delta V_{13} (T_{\text{ex}}(^{13}\text{CO}) + 0.91)}{1 - \exp \left[ -\frac{5.29}{T_{\text{ex}}(^{13}\text{CO})} \right]}$$

This function is shown in Fig. 4c. The central structure is not particularly clear in this map although quite a large column density is evident to the north of HD 200775. The low column density to the south is primarily due to optically thin  $^{13}\text{CO}$  but alternatively this may be a dilution effect resulting from the undersampling in the map. To the NE an arc of  $N(^{13}\text{CO}) > 2 \cdot 10^{16} \text{ cm}^{-2}$  is observed and this is what we interpret as the end of the outflow lobe.

In order to determine the properties of the high density region the contribution from any emission in front, or behind, along the line of sight must be removed. Outside this dense clump the average column density of  $^{13}\text{CO}$  is  $1.5 \cdot 10^{16} \text{ cm}^{-2}$ , the average within the clump is  $2.5 \cdot 10^{16} \text{ cm}^{-2}$ . Therefore a contribution of  $1 \cdot 10^{16} \text{ cm}^{-2}$  arises within the clump itself. Using a fractional abundance  $[^{13}\text{CO}]/[\text{H}_2] \sim 2 \cdot 10^{-6}$  and a projected path length of 0.03 pc (see following section) the average density  $n_{\text{H}_2} \sim 5.3 \cdot 10^4 \text{ cm}^{-3}$ .

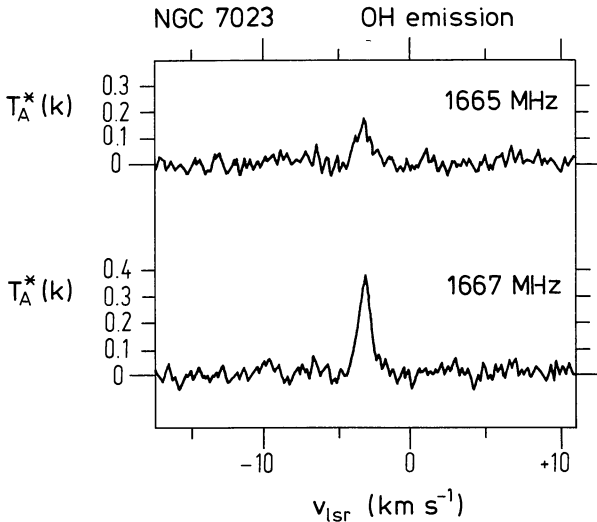


Fig. 6. Dwingeloo spectra of the OH lines at 1667 MHz and 1665 MHz showing emission from what is presumably circumstellar gas associated with HD 200775

In Fig. 5 contours of peak  $^{12}\text{CO}$  temperature and of  $^{13}\text{CO}$  column density are shown superposed on the red POSS plate of the nebula. A similar calculation to that above can be performed for the “doughnut” feature although the difference between the column density of  $^{13}\text{CO}$  in the ambient cloud and in the southern emission maximum is not obvious. However for the northern peak the contribution to the total column from material in the high-excitation ring is  $\sim 1.6 \cdot 10^{15} \text{ cm}^{-2}$  which for a projected pathlength of 0.3 pc gives  $n_{\text{H}_2} \sim 8.6 \cdot 10^2 \text{ cm}^{-3}$ , in close agreement with the density of the ambient cloud. The pathlength was estimated using Fig. 1a as a guide to the structure of inner radius 0.15 pc and outer radius 0.25 pc viewed edge on (see also Fig. 7).

#### 4. OH data

Spectra obtained on the 25-m Dwingeloo telescope in 1985 at 1667 MHz and 1665 MHz are shown in Fig. 6. The spectral resolution was 1.2 kHz or  $0.2 \text{ km s}^{-1}$  and the spatial resolution at this frequency is about  $30'$ . Integration was for 4 h. The ratio  $T_A^*(1667)/T_A^*(1665) = 2.4$  is in reasonable agreement with the equilibrium value of 3 expected for thermal emission from the circumstellar/interstellar gas. Our data differ from that of Lépine and Nguyen-Quang-Rieu (1975) in that these authors do not detect the 1665 MHz emission and in that their 1667 MHz spectrum appears to be composed of two components; a narrow feature probably due to emission from material at distances greater than 8 stellar radii, consistent with Fe II line observations (Weston, 1949), and a low intensity broad feature ( $\Delta v \sim 20 \text{ km s}^{-1}$ ) possible due to rotation of a disk-shaped envelope within 8 stellar radii of HD 200775. Our data do not have high enough angular resolution to resolve this wide velocity dispersion component. There is also no evidence of the OH absorption feature at  $-17 \text{ km s}^{-1}$  reported by Pankonin and Walmsley (1978), although this feature too may be unresolved by our beam.

#### 5. Discussion

In order to discuss the structure and energetics of this source in more detail, it is necessary to summarize the evolutionary stages of

an expanding circumstellar shell. Castor et al. (1975) describe this evolution in four major phases. Initially there is a free expansion of the stellar wind at velocity  $V_*$ , lasting only a few hundred years. This is followed by an adiabatic expansion of a few thousand years, a “snowplough” phase which lasts for most of the lifetime of the star and which is due to strong radiative cooling of the gas resulting in the build up of the thin, cold shell. Finally there is a dissipation phase as the shell relaxes and the flow tends towards a steady state. The long-enduring snowplough phase involves four zones of activity. Close to the star is a region of supersonic stellar wind with further out a hot, almost isobaric region in which the shocked wind is mixed with a little of the swept-up interstellar gas. At the end of this high temperature zone lies a thin, dense, cold compressed shell of swept-up material expanding at a velocity  $V_f$ . Most of the interstellar material pushed out from the hot outflowing zone lies in this region. Beyond the shell is the ambient, as yet unaffected, molecular cloud of density  $n_0 \text{ cm}^{-3}$ . The majority of the energy lost from the hot zone is used in maintaining the dense shell so that analysis of the molecules observed in this shell can be used to derive values for parameters in other parts of the source.

Before proceeding to interpret the maps of the previous section it is also necessary to define a geometry for the source. This is represented in Fig. 7 where HD 200775 has swept out a cavity of radius  $R_s$  into the interstellar gas, of density  $n_0$ . The outflow is not isotropic but is somehow confined into two lobes although in certain circumstances monopolar flows exist and have been observed, only one of which appears clearly in our data. The thin, dense shell postulated by Castor et al. has dimensions of  $x$ ,  $y$ , and  $z$  and an average density of  $n_s$  which is higher than  $n_0$ . In order to simplify the model the outflow lobe is assumed to have the same opening angle in  $y$  as in  $x$  and so the distance  $x$  equals  $y$  and the projected diameter of the dense shell  $x'$  and  $y'$  can be used to determine the angle  $i$  of the fragment to the perpendicular to the line of sight. By this method using the  $1.4 \cdot 10^{16} \text{ cm}^{-2}$  contour of Fig. 4c as an estimate of the fragment size the following parameters are deduced:

$$\begin{aligned} R_s &= 0.45 \text{ pc}, \\ V_f &= 16.2 \text{ km s}^{-1}, \\ i &= 21.7^\circ (\sim 20^\circ \text{ allowing for the uncertainties}) \\ x &= y = 0.7 \text{ pc}, \end{aligned}$$

assuming a distance of 350 pc to HD 200775. Careful analysis of Fig. 3b in the line wings down to  $T_A^*$  of 0.5 K yields peak velocities  $V_f'$  of about  $6 \text{ km s}^{-1}$  which allowing for projection gives  $V_f$  above.

To establish the mass of material swept-up in the shell some idea of the thickness of the shell ( $z$ ) is required in order to obtain the volume. A value of  $z = 0.01 \text{ pc}$  has been used, the justification of which appears later in this section. At an angle of  $21.7^\circ$  the projected pathlength ( $z'$ ) is 0.03 pc which leads to an average molecular hydrogen density through the dense shell of  $n_{\text{H}_2} \sim 5 \cdot 10^4 \text{ cm}^{-3}$ . Because CS has been detected from this region by Elmegreen and Elmegreen (1978) and the thermalization density for this species is  $\sim 10^6 \text{ cm}^{-3}$  (see Silk, 1985) it is likely that clumps of high density gas are present within the shell fragment. The total derived mass of material in the shell is  $M_s \sim 10 M_\odot$  with a total kinetic energy of  $E = \frac{1}{2} M_s V_f^2 = 2.5 \cdot 10^{46} \text{ erg}$  per lobe. It is useful in dealing with these objects to define a dynamic age to the outflow as  $\tau = R_s/V_f = 2.7 \cdot 10^4 \text{ yr}$  and to compare the mechanical luminosity of the flow  $L_f = 2E/\tau \approx 15 L_\odot$ , assuming an equal KE in the other lobe, with the total luminosity of the exciting source, in this case a B3 IV star with  $L_* \sim 2.5 \cdot 10^3 L_\odot$ . Thus the outflow process is using only 0.6% of the total available stellar luminosity. Calculating

NGC 7023

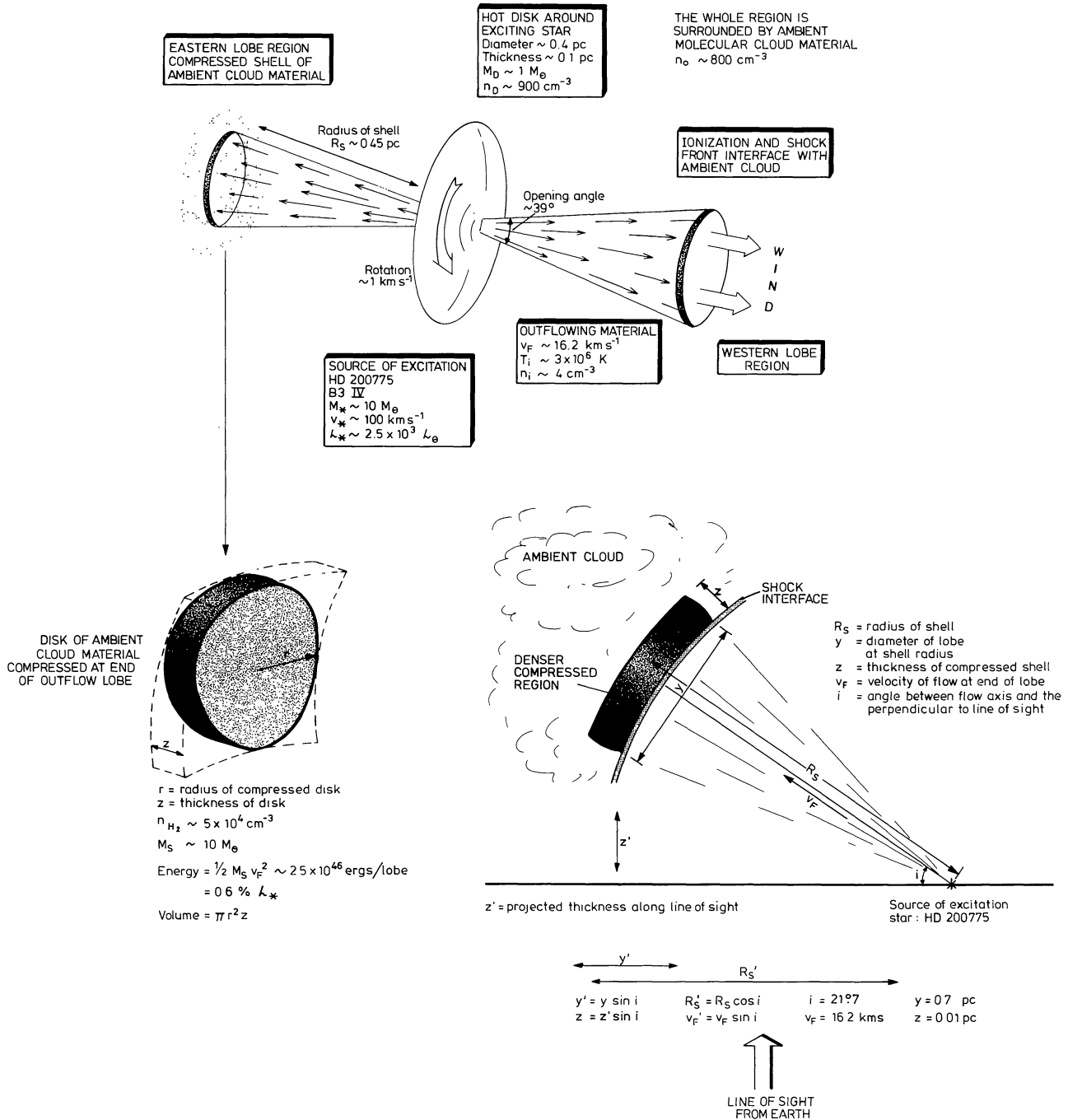


Fig. 7. Schematic illustration of the geometry involved in the interpretation suggested in the text for the gas emission observed near NGC 7023

the momentum in the flow, and using a stellar wind velocity  $V_* = 100 \text{ km s}^{-1}$  typical of early B types gives a mass loss rate

$$M_* \sim \frac{M_s V_f}{V_* \tau} \sim 5.8 \cdot 10^{-5} M_\odot \text{ yr}^{-1} \text{ or } 10^{-4.2} M_\odot \text{ yr}^{-1}.$$

which is typical of bipolar-outflow sources (Bally and Lada, 1983), but much larger than that expected for a B star.

The derived parameters can be checked by substitution in the equations for interstellar bubbles given by Castor et al. The radius of the shell should be

$$R_s(t) = 5.33 \cdot 10^{-3} \left[ \frac{\dot{M}_* V_*^2}{n_0} \right]^{0.2} t^{0.6} \text{ pc}$$



with  $M_* = M_\odot \text{ yr}^{-1}$ ;  $V_*$  in  $\text{km s}^{-1}$ ,  $n_0$  in  $\text{cm}^{-3}$ , and  $t$  in yr. For an ambient initial cloud density of  $2 \cdot 10^3 \text{ cm}^{-3}$ ,  $R_s = 0.5 \text{ pc}$  at  $2.7 \cdot 10^4 \text{ yr}$ , in reasonable agreement with the observed value. The temperature within the hot, outflow lobe can also be derived as can the average atomic density near the centre of the flow (i.e.: about  $0.25 \text{ pc}$  from HD 200775).

$$T_i = 1.24 \cdot 10^7 \frac{n_0^{2/35} [M_* V_*^2]^{18/35}}{t^{6/35}} \text{ K} \sim 3 \cdot 10^6 \text{ K}$$

and

$$n_i = 46.6 \frac{n_0^{19/35} [M_* V_*^2]^{16/35}}{t^{22/35}} \text{ cm}^{-3} \sim 4 \text{ cm}^{-3}.$$

The thickness of the shell can be determined from a calculation of the column density in the shell

$$N_s(t) = 5.52 \cdot 10^{15} n_0^{0.8} [M_* V_*^2]^{0.2} t^{0.6} \text{ cm}^{-2} \sim 9.9 \cdot 10^{20} \text{ cm}^{-2}$$

and requiring that the average density of molecular hydrogen should be  $5 \cdot 10^4 \text{ cm}^{-3}$ , in this manner  $z \simeq 0.01 \text{ pc}$  which supports the value used earlier in the calculations.

At this point we can summarize the model as follows: a B3IV type star of  $L_* \sim 2.5 \cdot 10^3 L_\odot$  and stellar wind velocity  $V_* \sim 100 \text{ km s}^{-1}$  somehow undergoes a mass loss at a rate of  $5.8 \cdot 10^{-5} M_\odot \text{ yr}^{-1}$  into bipolar lobes. These lobes are observed now to have dynamic age of  $2.7 \cdot 10^4 \text{ yr}$ , an internal atomic density of  $4 \text{ cm}^{-3}$  and temperature of  $3 \cdot 10^6 \text{ K}$ . At the ends of the lobes, which were expanding into an ambient molecular cloud of density  $2 \cdot 10^3 \text{ cm}^{-3}$  at a velocity of  $16 \text{ km s}^{-1}$ , is a swept-up shell of material of average density  $5 \cdot 10^4 \text{ cm}^{-3}$ . The energy required to maintain this shell is about  $5.0 \cdot 10^{46} \text{ ergs}$  which represents  $0.6\%$  of the energy available from the stellar luminosity.

The mechanism for driving this outflow is not easy to explain because the evidence for expansion of a stellar wind from HD 200775 using  $\text{H}\gamma$  to  $\text{H}\epsilon$  lines (Strom et al., 1972) shows a steep decrease in velocity with radial distance when compared to the  $\text{H}\beta$  profile which arises further from the star. Further evidence of little expansion at distances greater than 3 stellar radii is seen from  $\text{Fe II}$  lines (Herbig, 1960; Weston, 1949) which appear to have the same low velocity as the star. However this is only evidence for a lack of significant expansion along the line of sight where the observations reported here have detected a density gradient in the ambient cloud surrounding the central star. Most of the expansion of the stellar wind would be directed along the lobe directions which are about  $20^\circ$  to the line of sight and do not show much change in the radial velocities (a factor of 3 decrease due to projection).

This high-excitation ring of gas and dust is evident in other publications. Milkey and Dyck (1973) made multi-colour photometry of the source and suggested that the infrared excess observed is due to free-free emission from an ion plasma in a circumstellar location and that substantial opacity in emission is present reaching  $\tau \sim 3$  at  $10 \mu\text{m}$ . Viotti (1976) explains an apparent deficiency in UV energy for  $\lambda < 1600 \text{ \AA}$  with respect to normal stars as being due to line blocking in an extended opaque atmosphere but Witt and Cottrell (1980a) disagree and claim that the UV energy is normal but that the  $2200 \text{ \AA}$  feature is depleted. Altamore et al. (1980) contradict Milkey and Dyck by explaining that the IR emission is consistent with thermal dust emission from a radius of  $3 \cdot 10^{14} \text{ cm}$  and an ionized mass outflow of  $\sim 2.3 \cdot 10^{-9} M_\odot \text{ yr}^{-1} / \text{km s}^{-1}$  can be determined. The far-IR observations of Whitcomb et al. (1981) show the northern maximum of the ring at both  $55 \mu\text{m}$  and  $125 \mu\text{m}$  which confirms this point as a density enhancement. They derive a total atomic density of  $1-3 \cdot 10^3 \text{ atoms cm}^{-3}$  in the structure.

Figure 7 also contains a schematic representation of the ring observed in  $^{12}\text{CO}$  and  $^{13}\text{CO}$ . The parameters derived in the previous section lead to a mass  $M_D \sim 1 M_\odot$ . Because this density agrees well with that of the ambient cloud perhaps it is not strictly correct to view the structure as a density-enhanced disk, but more as a region of the ambient cloud unaffected by the directional outflows but possessing a kinetic (and  $^{13}\text{CO}$  excitation) temperature enhancement due to its proximity to HD 200775. This material may be part of the original gravitationally collapsed, cloud out of which the B star was created; in which case the chemical composition may be different from that in the dense shell region. Witt and Cottrell (1980) suggest that the radius of the Strömgren sphere for this star may be  $\sim 100''$  (which corresponds to the inner radius of our feature) which would imply  $\sim 20-40 \text{ atoms cm}^{-3}$  inside this sphere. The density into which this sphere is expanding can be calculated from Eq. (5.15) in Dyson and Williams (1980), altering units to

$$R_{ss} = 3.44 \cdot 10^{-16} [S_* T_e^{3/4}]^{1/3} n_H^{-2/3} \text{ pc}$$

where  $T_e$  is the electron temperature, usually in the range  $5 \cdot 10^3 \text{ K}$  to  $10^4 \text{ K}$ , and  $S_*$  is the rate at which ionizing photons are leaving the star. For a typical B star,  $S_*$  is  $2 \cdot 10^{47} \text{ s}^{-1}$  so that making  $R_{ss} = 0.15 \text{ pc}$  requires densities in the range  $1.2-1.6 \cdot 10^3 \text{ cm}^{-3}$  which agrees with our estimate for the ambient cloud density. This confirms our supposition that the feature is a high-excitation ridge, the edge of the Strömgren sphere, and not a density ridge.

A variety of models exist attempting to explain the production mechanisms for bipolar lobes using accretion disks (Snell et al., 1981; Elmegreen and Morris, 1979), interstellar nozzles (Cantó et al., 1981), anisotropic density distribution (Königl, 1982) or viscosity coupling (Calvet et al., 1981; Cantó et al., 1980) or some combination of these. Whatever model is necessary must satisfy the following criteria derived from the present observations:

1. the outflow appears collimated, not necessarily very strongly, into two opposite flows.
2. the source energy is usually sufficient to maintain the outflows provided an efficient process converts radiant luminosity to mechanical luminosity.

*Acknowledgements.* The National Radio Astronomy Observatory is operated by Associated Universities, Inc., under contract with the U.S. National Science Foundation. Support from the National Science Foundation to the University of Minnesota via grant NSF/AST 7921812 is gratefully acknowledged. The Netherlands Foundation for Radio Astronomy (SRZM) is supported by the Netherlands Organisation for Advancement of Pure Research (ZWO).

## References

- Altamore, A., Baratta, G.B., Cassatella, A., Grassdalen, G.L., Persi, P., Viotti, R.: 1980, *Astron. Astrophys.* **90**, 290  
 Bally, J., Lada, C.J.: 1983, *Astrophys. J.* **265**, 824  
 Calvet, N., Cantó, J., Rodriguez, L.F.: 1981, *Bull. Amer. Astron. Soc.* **13**, 784  
 Cantó, J., Rodriguez, L.F.: 1980, *Astrophys. J.* **239**, 982  
 Cantó, J., Rodriguez, L.F., Barral, I.F., Carral, P.: 1981, *Astrophys. J.* **244**, 102  
 Castor, J., McCray, R., Weaver, R.: 1975, *Astrophys. J.* **200**, L107

- Dyson, J.E., Williams, D.A.: 1980, in *The Physics of the Interstellar Medium*, Manchester University Press, p. 83
- Elmegreen, D.M.: 1982, in *Giant Molecular Clouds*, eds. P.M. Solomon, M.G. Edmunds, Pergamon Press, p. 231
- Elmegreen, D.M., Elmegreen, B.G.: 1978, *Astrophys. J.* **220**, 510
- Elmegreen, B.G., Morris, M.: 1979, *Astrophys. J.* **229**, 593
- Gezari, D.Y., Schmitz, M., Mead, J.M.: 1984, Far-IR Supplement Catalog of IR Observations, NASA Ref. Publ. 1119
- Herbig, G.H.: 1960, *Astrophys. J. Suppl.* **6**, 337
- Johnson, H.M.: 1968, in *Stars and Stellar Systems*, VII, p. 65
- Königl, A.: 1982, *Astrophys. J.* **261**, 115
- Kutner, M.L., Machnik, D.E., Tucker, K.D., Dickman, R.L.: 1980, *Astrophys. J.* **237**, 734
- Kutner, M.L., Ulrich, B.L.: 1981, *Astrophys. J.* **250**, 341
- Lepine, J.R.D., Nguyen-Quang-Rieu: 1975, *Astron. Astrophys.* **36**, 496
- Loren, R.B., Vanden Bout, P.A., Davis, J.H.: 1973, *Astrophys. J. Letters* **185**, L67
- Mendoza, E.E.: 1958, *Astrophys. J.* **128**, 207
- Milkey, R.W., Dyck, H.M.: 1973, *Astrophys. J.* **181**, 833
- Myers, P.C., Linke, R.A., Benson, P.J.: 1983, *Astrophys. J.* **264**, 517
- Ney, E.P., Hatfield, B.F., Gehrz, R.D.: 1980, *Proc. Natl. Acad. Sci.* **77**, 14
- Pankonin, V., Walmsley, C.M.: 1978, *Astron. Astrophys.* **67**, 129
- Silk, J.: 1985, Les Houches Lectures (1983) (in press)
- Snell, R.L., Loren, R.B., Plambeck, R.L.: 1980, *Astrophys. J.* **239**, 217
- Strom, S.E., Strom, K.M., Yost, I., Carrasco, L., Grasdalen, G.: 1972, *Astrophys. J.* **173**, 353
- Van Houten, C.J.: 1961, *Bull. Amer. Inst. Neth.* **509**, 1 (p. 32)
- Vanysek, V.: 1969, *Vista Astron.* **11**, 189
- Viotti, R.: 1964, *Mem. Soc. Astr. Ital. Nuova Ser.* **40**, 75
- Viotti, R.: 1976, *Astron. Astrophys.* **51**, 376
- Weston, E.B.: 1949, *Publ. Astron. Soc. Pacific* **61**, 256
- Weston, E.B.: 1953, *Astrophys. J.* **58**, 48
- Whitcomb, S.E., Gatley, I., Hildebrand, R.H., Keene, J., Sellgren, K., Werner, M.W.: 1981, *Astrophys. J.* **246**, 416
- Witt, A.N., Cottrell, M.J.: 1980a, *Astrophys. J.* **235**, 899
- Witt, A.N., Cottrell, M.J.: 1980b, *Astron. J.* **85**, 22